Journal of Zhejiang University-SCIENCE A (Applied Physics & Engineering)
ISSN 1673-565X (Print); ISSN 1862-1775 (Online)
www.zju.edu.cn/jzus; www.springerlink.com
E-mail: jzus@zju.edu.cn

Deflection analysis of reinforced concrete beams strengthened with carbon fibre reinforced polymer under long-term load action

Mykolas DAUGEVIČIUS[†], Juozas VALIVONIS, Gediminas MARČIUKAITIS

(*Department of Reinforced Concrete and Masonry Structures, Vilnius Gediminas Technical University, Saulėtekio Ave. 11, LT-10223 Vilnius, Lithuania*)

[†]E-mail: mykolas.daugevicius@vgtu.lt

Received Nov. 17, 2011; Revision accepted Feb. 27, 2012; Crosschecked July 9, 2012

Abstract: This paper presents the results of an experimental research on reinforced concrete beams strengthened with an external carbon fibre reinforced polymer (CFRP) layer under long-term load action that lasted for 330 d. We describe the characteristics of deflection development of the beams strengthened with different additional anchorages of the external carbon fibre composite layer during the period of interest. The conducted experiments showed that the additional anchorage influences the slip of the external layer with respect to the strengthened element. Thus, concrete and carbon fibre composite interface stiffness decreases with a long-term load action. Therefore, the proposed method of analysis based on the built-up-bars theory can be used to estimate concrete and carbon fibre composite interface stiffness in the case of long-term load.

Key words: Carbon fibre composite, Beam strengthening, Beam deflection, Long-term load, Bending stiffness, Concrete and carbon fibre composite interface stiffness, Effective inertia moment

doi:10.1631/jzus.A1100317 **Document code:** A **CLC number:** TU411

1 Introduction

Carbon fibre reinforced polymer (CFRP) has been increasingly applied to strengthen and retrofit the elements of damaged structures. From a number of research endeavours, the introduction of design recommendations and effective application of the developed method for the strengthening technology, prove the prospective and practical use of CFRP in the near future. Strengthening technologies that apply CFRP have improved, and are close to perfection, in many countries. Strengthening building structures with carbon fibre composites are generally achieved by creating an external layer of the composite on the structure. It has been proved experimentally that the concrete and external reinforcement interface is not absolutely stiff (Weimer and Haupert, 2000; Ferrier and Hamelin, 2002; Gao *et al*., 2003; Davis *et al*., 2004; Valivonis, 2006; Benzaid *et al*., 2008; Ferrier *et al*., 2010).

It has been determined experimentally that a concrete layer impregnated with epoxy glue is formed along the concrete and carbon fibre composite interface (Marchukaitis *et al*., 2007). The physical and mechanical properties of this layer are better than those of concrete for the member to be strengthened. Concrete tensile strength in this zone is increased, which improves resistance to cracking. The experiments showed that the first vertical crack appeared above the impregnated concrete layer. Because of the growth of external forces, increasing shear stresses above the concrete and composite interface causes horizontal cracking. Therefore, the concrete layer above the concrete and composite interface is cracked significantly (Marchukaitis *et al*., 2007; Marčiukaitis *et al*., 2010). The formation of cracks and the tension stiffening effect depend on the concrete and steel bar interface stiffness and the concrete and FRP element interface stiffness (Lee *et al*., 1999). Because of a long-term load action, shear creep occurs in the interface aforementioned, and the composite layer slips with respect to the reinforced concrete of the strengthened member. The slip of the composite layer and concrete nonlinear creep (Balevičius and Dulinskas, 2010) reduce the stiffness of the strengthened member and causes additional deflection to occur.

The duration and level of the long-term load have a significant influence on the behaviour of strengthened structures. Wang and Li (2006a; 2006b) experimentally investigated reinforced concrete beams strengthened with carbon fibre composites and subjected to a long-term load action, which showed that strengthening becomes less effective as the load level of concrete structures increases.

To enhance the strengthening effect using carbon fibre composites, various methods of anchoring the composite layer have been proposed. Bolted steel plates were used as additional mechanical anchors in beams with prestressed CFRP (Diab *et al.*, 2009). Non-metallic anchor systems with carbon fibre clamps were investigated to replace the steel anchors (Xiong *et al.*, 2007; Kim *et al.*, 2008a; 2008b). Skuturna *et al.* (2008) showed that additional anchors for the composite layer change the beam failure characteristics, increase the load carrying capacity, and decrease the beam deflection.

The development of beam deflection, subjected to a long-term static action, depends on the value of the reinforcement ratio of the cross-sectional carbon fibre composites. Tan and Saha (2006) revealed that deflection decreased from 23% to 33% when the reinforcement ratio of carbon fibre composites increased from 0.64% to 1.92%. An experiment with old-new concrete composite beams showed that deflections mostly increase as a result of creep and shrinkage in the new concrete; however, the influence of slip strains on deflection is small (Wang *et al.*, 2011).

Diab *et al.* (2009) pointed out that the greatest deformation of shear creep developed in the zones subjected to the highest shear stress, i.e., at the ends of the glued fibre.

It is expedient in the analysis of deflecting multilayer beams to allow for additional deflection caused by inter-displacements of the layers. The calculation results of the analysis of reinforced concrete beams strengthened with carbon fibre composites (Benyoucef *et al.*, 2007a; 2007b) show that a slip between the layers and the intensity of corresponding shear stresses depend on the axial stiffness of the composite layer.

However, most analyses of the deflection of reinforced concrete beams strengthened with carbon fibre composites (Tan and Saha, 2006; Fib Task Group 9.3, 2001) do not take into account the concrete and carbon fibre composite interface stiffness. Therefore, in the case of a long-term load action, the influence of shear creep deformations on beam deflection is completely neglected. According to regression analysis results, a nonlinear model for concrete and fibre reinforced plastic interface behaviour has been proposed (Dai *et al.*, 2005).

Little research has focused on the influence of a long-term load on the behaviour of the strengthened structure. An inadequate number of investigations determine the influence of long-term load magnitude and stress strain state before strengthening, as well as various anchor methods on the behaviour of structures strengthened with carbon fibre composites during the long-term load action. Considering the above information, experimental and theoretical investigations into reinforced concrete beams strengthened with carbon fibre composites subjected to a long-term load action were performed and are reported in this paper.

2 Deflection analysis

Formulae for deflection analysis of beams destined for solid cross-section members cannot be used for layered members. Slips that occurred between the layers increase beam deflection. Because of the long-term load action, longitudinal shear creep deformations appear in the concrete and carbon fibre composite interface and result in an increase in beam deflection. A method for deflection analysis of beams strengthened with carbon fibre composites is proposed based on the built-up-bars (Rzhanitsyn, 1986; Marčiukaitis *et al.*, 2006) theory that the long-term load action accounts for changes in the interface stiffness of the layers.

The deflection of a beam loaded with uniformly distributed load p with a span length l can be calculated by the following modified expression:

$$\omega(t)=\frac{5pl^4}{384E_{\text{eff}}(t)I_{\text{eff}}(t)}+\frac{p}{\lambda(t)^4\cdot D(t)}\left(\frac{1}{\text{ch}\lambda(t)\cdot l}+\frac{\lambda(t)^2\cdot l^2}{2}-1\right), \tag{1}$$

where t is the time coordinate, λ is the parameter that evaluates the alteration of bond stiffness, and $E_{\mathrm{eff}}(t)I_{\mathrm{eff}}(t)$ is the effective bending stiffness.

The deflection of a strengthened beam loaded with two concentrated loads (Fig. 1a) can be used to estimate the influence of a long-term load using the following modified expression:

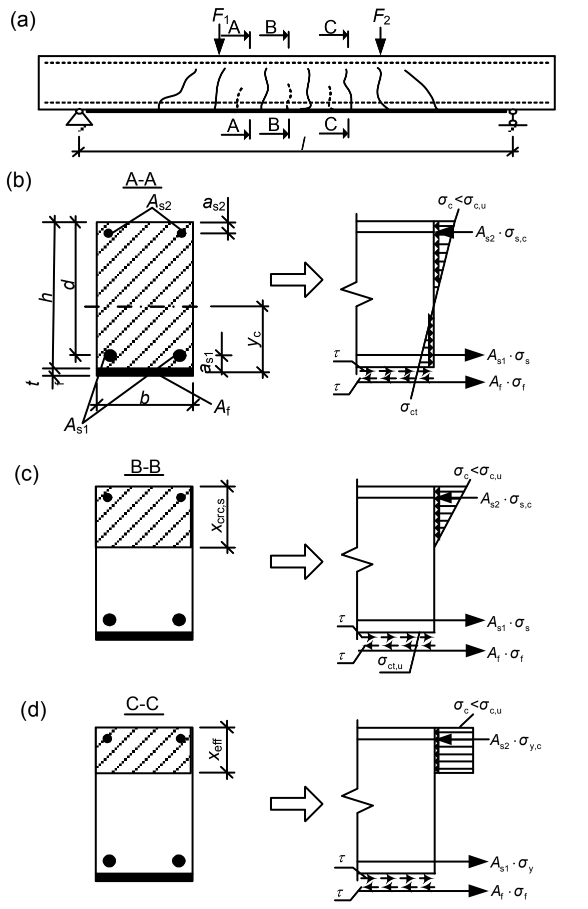

A_f: cross sectional area of a carbon fibre composite;
A_{s1}: cross section of tensioned reinforcement;
A_{s2}: cross section of compressed steel bars;
y_c: distance to the centre of the reinforced concrete section;
x_{eff}: height of the compressed concrete zone at the highest vertical crack section;
$x_{\mathrm{crc,s}}$: height of the compressed concrete zone of a newly opened crack;
b: width of a beam cross section; d: effective height of a cross section;
h: height of a beam cross section; l: span length of the beam;
σ_c: concrete compression stress; $\sigma_{c,u}$: ultimate σ_c;
σ_{ct}: concrete tensile stress; $\sigma_{ct,u}$: ultimate σ_{ct};
σ_f: tensile stress of CFRP; σ_s: tensile stress of steel bars;
σ_y: yielding stress; $\sigma_{y,c}$: steel yielding stress under compression;
τ: shear stresses in concrete and carbon fiber composite interface

Fig. 1 Evaluation of the bending stiffness of cracked beam sections
(a) Loading scheme; (b) Non-cracked cross section A-A; (c) Section B-B with a newly opened crack after strengthening; (d) Cracked section C-C with the highest vertical crack

$$\omega(t)=\frac{Ml^2}{8E_{\mathrm{eff}}(t)I_{\mathrm{eff}}(t)}+\frac{M}{D(t)}\left(\frac{\mathrm{ch}\left(0.5\lambda(t)l\right)-1}{\lambda(t)^2\mathrm{ch}\left(0.5\lambda(t)l\right)}\right), \quad (2)$$

where M is the acting moment, and $1/D(t)$ can be expressed as follows:

$$\frac{1}{D(t)}=\frac{1}{E_{\mathrm{c,eff}}(t)I_{\mathrm{c,eff}}(t)}-\frac{1}{E_{\mathrm{eff}}(t)I_{\mathrm{eff}}(t)}. \quad (3)$$

The parameter that evaluates the alteration of bond stiffness during a long-term load action is described as follows:

$$\lambda(t)=\sqrt{\xi_{\mathrm{k}}(t)\gamma(t)}, \quad (4)$$

where $\gamma(t)$ is a parameter that indicates the influence of longitudinal shear forces during a long-term loading period on the interface stiffness, and is evaluated using seven or eight formulae based on the loading conditions. The parameter $\xi_{\mathrm{k}}(t)$ is calculated as

$$\xi_{\mathrm{k}}(t)=\frac{bG_{\mathrm{c,eff}}(t)}{z(t)}, \quad (5)$$

where b is the width of a beam cross section, $G_{\mathrm{c,eff}}(t)$ is the effective shear modulus of a concrete and carbon fibre composite interface, and z is the distance between a cross section of the reinforced concrete element and a cross section of carbon fibre composites.

The effective bending stiffness is as follows:

$$E_{\mathrm{eff}}(t)I_{\mathrm{eff}}(t)=\gamma(t)E_{\mathrm{c,eff}}(t)I_{\mathrm{c,eff}}(t)\cdot\frac{E_{\mathrm{c,eff}}(t)A_{\mathrm{c,eff}}(t)\cdot E_{\mathrm{f}}A_{\mathrm{f}}}{E_{\mathrm{c,eff}}(t)A_{\mathrm{c,eff}}(t)+E_{\mathrm{f}}A_{\mathrm{f}}}, \quad (6)$$

where $E_{\mathrm{c,eff}}(t)$ is an effective secant modulus of concrete, $I_{\mathrm{c,eff}}(t)$ and $A_{\mathrm{c,eff}}(t)$ are an effective moment of inertia and an effective cross section of the reinforced concrete element, respectively, E_{f} is the modulus of elasticity of the carbon fibre composite, and A_{f} is a cross sectional area of the carbon fibre composite.

If a beam is strengthened and concrete hardening age reaches 28 d, then

$$\gamma(t)=\frac{1}{E_{\mathrm{c,eff},t_0}A_{\mathrm{c,eff},t_1}}+\frac{\phi_{\mathrm{c},t_0}}{2E_{\mathrm{c,eff},t_0}A_{\mathrm{c,eff},t_0}}+\frac{\phi_{\mathrm{c},t_1}}{2E_{\mathrm{c,eff},t_0}A_{\mathrm{c,eff},t_1}}$$
$$+\frac{z_{t_0}^2}{E_{\mathrm{c,eff},t_0}I_{\mathrm{c,eff},t_1}}+\frac{z_{t_0}^2\phi_{\mathrm{c},t_0}}{2E_{\mathrm{c,eff},t_0}I_{\mathrm{c,eff},t_0}}+\frac{z_{t_0}^2\phi_{\mathrm{c},t_1}}{2E_{\mathrm{c,eff},t_0}I_{\mathrm{c,eff},t_1}}$$
$$+\frac{1}{E_{\mathrm{f},t_0}A_{\mathrm{f},t_1}}+\frac{\phi_{\mathrm{c},t_0}}{2E_{\mathrm{f},t_0}A_{\mathrm{f},t_0}}+\frac{\phi_{\mathrm{c},t_1}}{2E_{\mathrm{f},t_0}A_{\mathrm{f},t_1}},\tag{7}$$

where $\phi_{\mathrm{c,t}}$ is the characteristic of concrete creep.

If a beam is strengthened and loaded after more than 28 d of concrete hardening, the parameter that indicates the influence of longitudinal shear forces during a long-term loading period on the alteration of interface stiffness is as follows:

$$\gamma(t)=\frac{k_1}{E_{\mathrm{c,eff},t_0}A_{\mathrm{c,eff},t_0}}+\frac{k_2}{E_{\mathrm{c,eff},t_0}A_{\mathrm{c,eff},t_1}}+\frac{k_1z^2}{E_{\mathrm{c,eff},t_0}I_{\mathrm{c,eff},t_0}}$$
$$+\frac{k_2z^2}{E_{\mathrm{c,eff},t_0}I_{\mathrm{c,eff},t_1}}+\frac{k_1}{E_{\mathrm{f},t_0}A_{\mathrm{f},t_0}}+\frac{k_2}{E_{\mathrm{f},t_0}A_{\mathrm{f},t_1}},\tag{8}$$

where k_1 and k_2 are coefficients that evaluate the concrete age and are calculated with expressions proposed by Livshyc (1976).

The effective bending stiffness with an evaluated increment of longitudinal shear creep deformation can be calculated as follows:

$$E_{\mathrm{eff}}(t)I_{\mathrm{eff}}(t)=\frac{B_1(t)+B_2(t)+B_3(t)}{B_4}\cdot\frac{E_{\mathrm{c,eff},t}^2}{E_{\mathrm{c,eff},t}A_{\mathrm{c,eff},t}+E_{\mathrm{f}}A_{\mathrm{f}}},\tag{9}$$

where

$$B_1(t)=\phi_{\mathrm{c},t_0}\times A_{\mathrm{c,eff},t}I_{\mathrm{c,eff},t}\times(E_{\mathrm{f}}A_{\mathrm{f}}I_{\mathrm{c,eff},t_0}+z_{t_0}^2E_{\mathrm{f}}A_{\mathrm{f}}A_{\mathrm{c,eff},t_0}+E_{\mathrm{c,eff},t_0}A_{\mathrm{c,eff},t_0}I_{\mathrm{c,eff},t_0}),\tag{10}$$

$$B_2(t)=\phi_{\mathrm{c},t}\times A_{\mathrm{c,eff},t_0}I_{\mathrm{c,eff},t_0}\times(E_{\mathrm{f}}A_{\mathrm{f}}I_{\mathrm{c,eff},t}+z_{t_0}^2E_{\mathrm{f}}A_{\mathrm{f}}A_{\mathrm{c,eff},t}+E_{\mathrm{c,eff},t_0}A_{\mathrm{c,eff},t}I_{\mathrm{c,eff},t}),\tag{11}$$

$$B_3(t)=2A_{\mathrm{c,eff},t_0}I_{\mathrm{c,eff},t_0}\times(E_{\mathrm{f}}A_{\mathrm{f}}I_{\mathrm{c,eff},t}+z_{t_0}^2E_{\mathrm{f}}A_{\mathrm{f}}A_{\mathrm{c,eff},t}+E_{\mathrm{c,eff},t_0}A_{\mathrm{c,eff},t}I_{\mathrm{c,eff},t}),\tag{12}$$

$$B_4=2E_{\mathrm{c,eff},t_0}A_{\mathrm{c,eff},t_0}I_{\mathrm{c,eff},t_0}.\tag{13}$$

When a beam is strengthened and loaded after more than 28 d of concrete hardening, then the effective bending stiffness is as follows:

$$E_{\mathrm{eff}}(t)I_{\mathrm{eff}}(t)=\frac{B_{1,t}(t)+B_{2,t}(t)}{B_{3,t}}\cdot\frac{E_{\mathrm{c,eff},t}^2}{E_{\mathrm{c,eff},t}A_{\mathrm{c,eff},t}+E_{\mathrm{f}}A_{\mathrm{f}}},\tag{14}$$

where

$$B_{1,t}(t)=k_1A_{\mathrm{c,eff},t}I_{\mathrm{c,eff},t}\times(E_{\mathrm{f}}A_{\mathrm{f}}I_{\mathrm{c,eff},t_0}+z_{t_0}^2E_{\mathrm{f}}A_{\mathrm{f}}A_{\mathrm{c,eff},t_0}+E_{\mathrm{c,eff},t_0}A_{\mathrm{c,eff},t_0}I_{\mathrm{c,eff},t_0}),\tag{15}$$

$$B_{2,t}(t)=k_2A_{\mathrm{c,eff},t}I_{\mathrm{c,eff},t}\times(E_{\mathrm{f}}A_{\mathrm{f}}I_{\mathrm{c,eff},t}+z_{t_0}^2E_{\mathrm{f}}A_{\mathrm{f}}A_{\mathrm{c,eff},t}+E_{\mathrm{c,eff},t_0}A_{\mathrm{c,eff},t}I_{\mathrm{c,eff},t}),\tag{16}$$

$$B_{3,t}=E_{\mathrm{c,eff},t_0}A_{\mathrm{c,eff},t_0}I_{\mathrm{c,eff},t_0}.\tag{17}$$

It is necessary to evaluate the cracked region of a beam section as well as the shear of the concrete layer between the tensioned steel reinforcement and the external CFRP layers. The effective inertia moment of a cracked strengthened beam due to cracking of the tensioned layer is proposed as follows:

$$I_{\mathrm{c,eff}}(t)=\left(\frac{M_{\mathrm{crc}}}{M_{\mathrm{e}}}\right)^3\beta_2(t)I_{\mathrm{gros}}(t)+\left(\frac{M_{\mathrm{r,s}}}{M_{\mathrm{e}}}\right)^3\beta_1I_{\mathrm{crc}}(t)$$
$$-\left(\frac{M_{\mathrm{crc}}}{M_{\mathrm{e}}}\right)^3\beta_2(t)I_{\mathrm{crc}}(t)+I_{\mathrm{s}}(t)-\left(\frac{M_{\mathrm{r,s}}}{M_{\mathrm{e}}}\right)^3\beta_1I_{\mathrm{s}}(t),\tag{18}$$

where M_{crc} is the moment of cracking calculated by evaluating an increase in concrete tensile strength according to Marčiukaitis *et al.* (2010); $M_{\mathrm{r,s}}$ is the ultimate moment of the non-strengthened beam; M_{e} is the acting moment of the strengthened beam; $\beta_1=\frac{E_{\mathrm{f}}A_{\mathrm{f}}}{E_{\mathrm{s}}A_{\mathrm{s1}}}$; and, $\beta_2(t)=\frac{A_{\mathrm{f}}E_{\mathrm{f}}}{x_{\mathrm{eff}}(t)bE_{\mathrm{c}}(t)}$.

The inertia moment of the non-cracked cross section (section A-A in Fig. 1b) is as follows:

$$I_{\mathrm{gros}}(t)=bh^3/12+bh\left(h/2-y_{\mathrm{c}}(t)\right)^2+\alpha_{\mathrm{s2}}(t)A_{\mathrm{s2}}\left(h-y_{\mathrm{c}}(t)-a_{\mathrm{s2}}\right)^2+\alpha_{\mathrm{s1}}(t)A_{\mathrm{s1}}\left(y_{\mathrm{c}}(t)-a_{\mathrm{s1}}\right)^2,\tag{19}$$

where $\alpha_{s1}(t)=\alpha_{s2}(t)=E_s/E_{c,eff}(t)$. Other designations are shown in Fig. 1.

The inertia moment of the cracked section (C-C in Fig. 1d) is as follows:

$$I_{crc}(t)=bx_{eff}(t)^3/3+\alpha_{s2}(t)A_{s2}\left(x_{eff}(t)-a_{s2}\right)^2 +\alpha_{s1}(t)A_{s1}\left(d-x_{eff}(t)-a_{s1}\right)^2. \tag{20}$$

The inertia moment of a section with a newly opened crack (B-B in Fig. 1c) is as follows:

$$I_s(t)=bx_{crc,s}(t)^3/3+\alpha_{s2}(t)A_{s2}\left(x_{crc,s}(t)-a_{s2}\right)^2 +\alpha_{s1}(t)A_{s1}\left(d-x_{crc,s}(t)-a_{s1}\right)^2. \tag{21}$$

The height of the compressed concrete zone at the highest vertical crack section (C-C in Fig. 1d) $x_{eff}(t)$ can be calculated according to

$$x_{eff}(t)=d\left(\sqrt{\mu(t)^2+\mu(t)h/d}-\mu(t)\right). \tag{22}$$

The parameters are as follows:

$$\mu(t)=\mu_{s1}\alpha_{s1}(t)+\mu_{s2}\alpha_{s2}(t)+\mu_f\alpha_f(t), \tag{23}$$

$$\mu(t)h=2\left(\mu_{s1}\alpha_{s1}(t)d+\mu_{s2}\alpha_{s2}(t)d+\mu_f\alpha_f(t)(h-t_f/2)\right), \tag{24}$$

where $\mu_{s1}=\dfrac{A_{s1}}{bd}$, $\mu_{s2}=\dfrac{A_{s2}}{bd}$, and $\mu_f=\dfrac{A_f}{b(h+t_f/2)}$.

The effective secant modulus of concrete at different time intervals can be calculated by the adjusted effective modulus method:

$$E_{c,eff}(t)=E_{c,eff}(t_0)/\left(1+\chi\phi_c(t)\right), \tag{25}$$

where $E_{c,eff}(t_0)$ is the primary secant modulus of concrete and χ is the coefficient of ageing. Variation in creep over time can be calculated according to the Eurocode 2 recommendations (EN 1992-1, 2001).

3 Experimental research on strengthened reinforced concrete beams

Fourteen reinforced concrete beams were prepared for the experimental research. The objective of this research is to experimentally determine the influence of additional anchors on displacement of the external layer with respect to the strengthened element. The beams in the tensioned section zone were reinforced with 2×Φ12 mm (μ_s=1.29%) steel bars and were reinforced in the compressed section zone with 2×Φ8 mm steel bars. The yielding strength of the tensioned steel bars was $f_{s,y}$=318 MPa, and the ultimate strength was $f_{s,u}$=456 MPa. The yielding strength of compressed steel bars was $f_{s,y}$=420 MPa, and the ultimate strength was $f_{s,u}$=525.6 MPa. The compressive strength of concrete in the beams was f_c=30.1 MPa, the tensile strength was f_{ct}=3.46 MPa, and the modulus of elasticity was E_c=32.38 GPa. A carbon fibre tape with a width of 100 mm was used for strengthening. The tensile strength of the carbon fibre tape was $f_{f,t}$=1988 MPa, the modulus of elasticity was $E_{f,t}$=230 GPa, and the cross sectional area was $A_{f,t}$=0.1837 cm^2. The tensile strength of epoxy glue was $f_{e,t}$=32.6 MPa, the modulus of elasticity was E_e=1.8 GPa, and the shear modulus was G_e=1.58 GPa. The dimensions of the cross section of beams and anchor methods of the external carbon fibre composite layer are presented in Table 1.

Concrete beams reinforced with steel bars were strengthened according to the real working condition of the beams. Loading stages and strengthening time are described in Tables 2 and 3. Continuous carbon fibre fabric was placed using a dry system method. At times, the acting load could not be removed, but in general, the acting load must be decreased before strengthening. Considering these statements, several strengthening conditions of experimental beams were examined. Eight concrete beams reinforced with steel bars (B3S, B4S, B5S, B6S, B7S, B8S, B9S, and B10S) were loaded with long-term loads that reached 60% of the resistance of the non-strengthened beams. After 14 d of long-term load action, beams B3S, B4S, B5S, and B6S were strengthened with an external carbon fibre composite layer. The long-term load of the other four beams, B7S, B8S, B9S, and B10S, was increased up to 86% of the resistance of the non-strengthened control beams. After five days, the load was decreased to 52% of the resistance of the non-strengthened control beams, and the beams were strengthened. Beams B11S and B12S were strengthened without external load action.

Table 1 Characteristics of strengthened beams (unit: mm)

Beam	Section dimension $b\times h^*$	Strengthening scheme	Cross section
B1	104×198	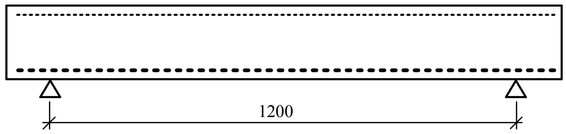	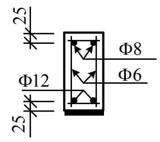
B2	105×201		
B3S	100×200	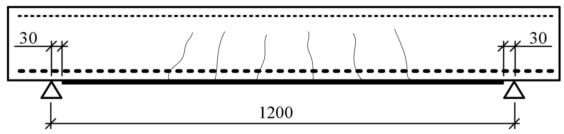	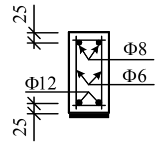
B4S	100×198		
B5S	101×199	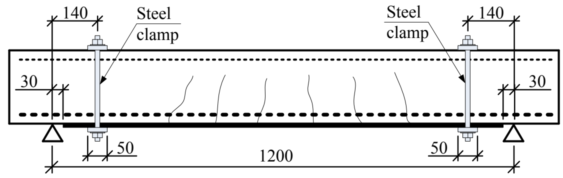	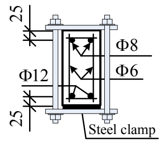
B6S	99×198		
B7S	100×198	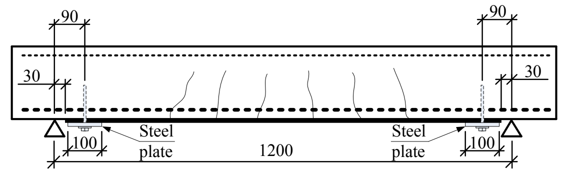	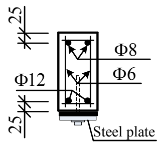
B8S	98×195		
B9S	100×201	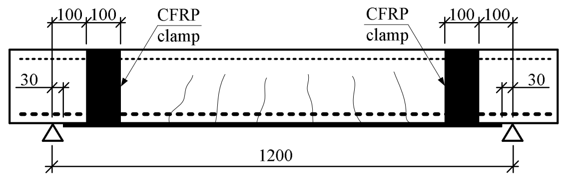	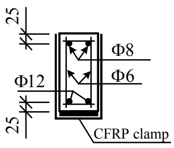
B10S	100×199		
B11S	102×199	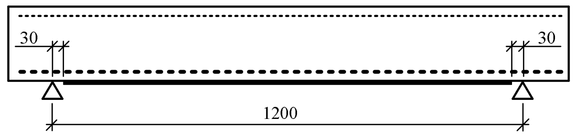	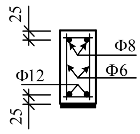
B12S	100×197		

* b and h are the width and height of a beam cross section, respectively

Table 2 Loading stages of beams B3S, B4S, B5S, and B6S

Beam	Additional anchorage type	t_0=0 d	t_1=14 d	t_2=29 d
B3S B4S B5S B6S	Steel clamp	Long-term load reached 60% of the resistance of non-strengthened beams	Beams were strengthened with CFRP	Load was increased up to 98% of the resistance of non-strengthened beams

Table 3 Loading stages of beams B7S, B8S, B9S, and B10S

Beam	Additional anchorage type	t_0=0 d	t_1=15 d	t_2=20 d	t_3=28 d	t_4=46 d
B7S B8S	Steel plate	Long-term load reached 60% of the resistance of non-strengthened beams	Long-term load increased up to 86% of the resistance of non-strengthened beams	Long-term load decreased to 52% of the resistance of non-strengthened beams	Beams were strengthened with CFRP	Load increased to 97% of the resistance of non-strengthened beams
B9S B10S	CFRP clamp					

The long-term load intensity of all strengthened beams reached 98% of the resistance of the non-strengthened control beams, which corresponded to 60% of the resistance of the strengthened beams. The external carbon fibre composite layer of beams B5S and B6S was also anchored with steel clamps. The external carbon fibre composite layer of beams B7S and B8S was also anchored with steel plates of 100 mm×100 mm, which were anchored into beam concrete. The external carbon fibre composite layer of beams B9S and B10S was additionally anchored with carbon fibre tape clamps of a 100-mm width. The external carbon fibre composite layer of beams B3S, B4S, B11S, and B12S did not have additional anchors.

During the long-term load experiment, the strengthened beams were loaded in pairs (Fig. 2). The arrangement of measurement devices for deflection, slip and deformations of the tensioned and compressed layers are presented in Fig. 3. Deformations were measured on the external compressed concrete layer, on the compressed layer with a steel bar, on the tensioned layer with steel bars, and on the external tensioned layer of carbon fibre composites. Longitudinal shear deformations across the concrete to carbon composite interface were measured by fixing shear measurement devices near the ends of the anchors of external carbon fibre composite layers. The distance from the point at which the slip was measured to the free end of CFRP laminate varied because additional anchor methods captured different areas of CFRP laminate. For the beams without additional CFRP laminate anchors, the slip was measured at the point that was 0.11 m from the free end of the CFRP laminate. For beams with additional steel plates, steel clamps and CFRP clamps, the slip was measured at the point which was 0.12, 0.14, and 0.17 m, respectively, from the free end of CFRP laminate. Beam deflection was measured in the middle of the span length. The external load was gradually increased by 5 kN until the long-term load level was reached. Deformations were measured after each increase in load level.

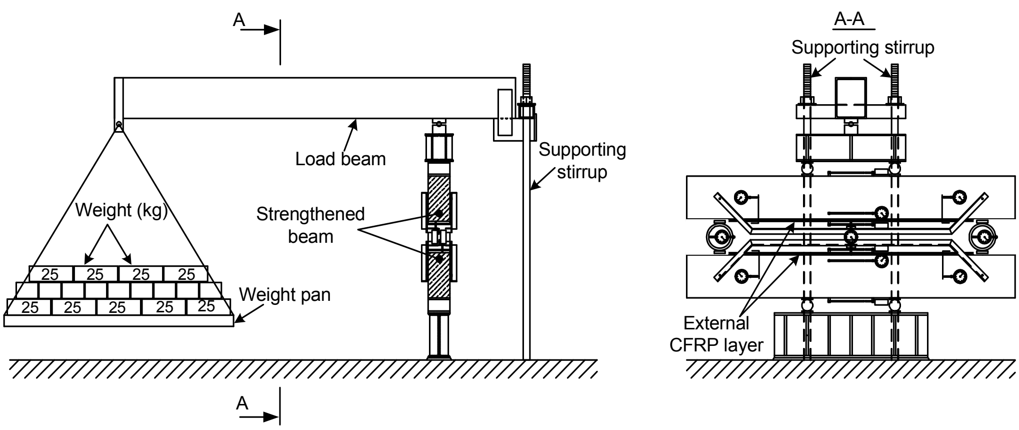

Fig. 2 Testing scheme of beams during a long-term loading

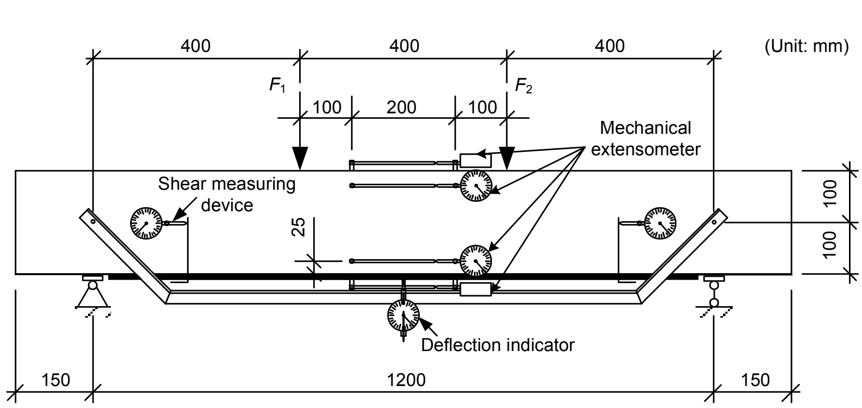

Fig. 3 Arrangement of deformation measurement devices on the experimental beam during a long-term loading

Concrete prisms were loaded for compression with long-term static loads at the same time as the beams. The cross sections of the prisms were 100 mm×100 mm, and they were 400 mm long. The long-term load intensity reached 60% of the compressive strength of the prisms. Longitudinal and transversal deformations were measured. The effective modulus of the elasticity of concrete was calculated according to long-term prism test results.

4 Analysis of longitudinal shear deformation evolution in concrete and carbon fibre composite interface

Experiments with short-term loads showed that concrete and carbon fibre composite interfaces were not stiff. This research proved that during a long-term loading, longitudinal shear deformations in concrete and carbon fibre composite interfaces increased significantly (Fig. 4). The slip of the external composite layer depends on the added anchors. Thus, the influence of additional anchors on the external composite layer was investigated during the experiment on the long-term load action.

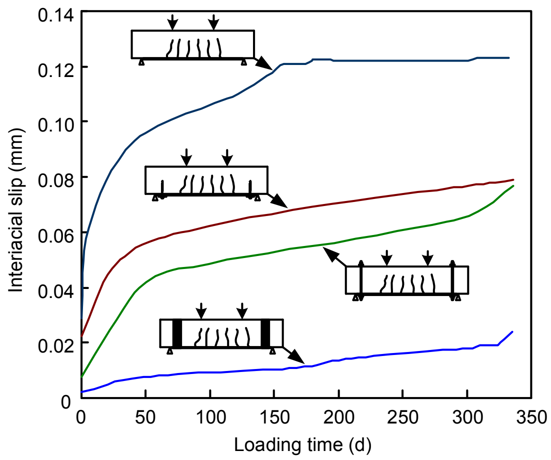

Fig. 4 Evolution of the CFRP layer slip with different anchoring methods

Additional anchorage of the external composite layer influenced the slip of the external layer during short-term and long-term loading experiments (Fig. 4). It was experimentally determined that the horizontal slip of the external CFRP layer at the beginning of the long-term load action in the beams where the external CFRP layer did not have additional anchors reached 0.029 mm. When the external CFRP layer had steel plates as additional anchors, the slip of the external CFRP layer was 24% lower (with respect to the beams where the external layer was not additionally anchored), and reached 0.022 mm. When the external CFRP layer was additionally anchored with steel clamps, the slip was 73% lower and reached 0.0078 mm. When the external CFRP layer was additionally anchored with carbon fibre clamps, the slip was 93% lower and reached 0.002 mm. During the long-term load action, the slip of the external CFRP layer increased. Longitudinal shear deformations rapidly increased during the first 50 d of the long-term load action. During this period, the slip of the external CFRP layer in the beams where the external CFRP layer was not additionally anchored was up to three times larger and reached 0.093 mm. When the external CFRP layer was additionally anchored with steel plates, steel clamps or carbon fibre composite clamps, the slip was up to 2.4 times (0.054 mm), 4.8 times (0.038 mm) or 3.6 times (0.0073 mm) larger, respectively, than at the beginning of the long-term load action period.

The analysis of experimental results showed that when the external carbon fibre composite layer was additionally anchored with carbon fibre clamps, the slip following the first 50 d of long-term load action was 12.7 times smaller than in the strengthened beams where the external CFRP layer was not additionally anchored. When the external layer was additionally anchored with steel plates and steel clamps, the slip was 1.72 and 2.4 times smaller, respectively.

At the end of long-term load action, the longitudinal slip of the external carbon fibre composite layer was 4.2 times (0.123 mm), 3.6 times (0.079 mm), 9.8 times (0.077 mm), or 12 times (0.024 mm) greater than the primary slip when the CFRP layer was not additionally anchored, additionally anchored with steel plates, additionally anchored with steel clamps or additionally anchored with carbon fibre clamps, respectively. This showed that the effectiveness of additional anchorage decreased during the long-term load action, and the horizontal slip of the external CFRP layer was the smallest when it was additionally anchored with carbon fibre clamps (Fig. 4). In this case, longitudinal shear deformations in the concrete and carbon fibre composite interface were 12 times lower than those in the beams in which the CFRP layer was not additionally anchored. Other anchoring methods did not have such influence (Fig. 4). Steel clamps do not have adhesion with the external surface of concrete, and they can move because of shear force action. Carbon fibre composite clamps have adhesion with the external surface of concrete and can effectively confine shear deformations in concrete and CFRP laminate interface.

5 Experimental deflection of the beams strengthened with carbon fibre composites

The experimental deflection results were analysed. Experimental research suggested that the deflection of the strengthened beams that were not previously loaded at the initial long-term load action period was 12% higher than that of the beams strengthened with the external load action (Fig. 5). The deflection of the beams that prior to strengthening were externally loaded was lower, because the concrete structure in the compressed zone was changed, and creep deformations developed along with a change in the concrete modulus of elasticity due to the long-term loading.

However, over time, the deflection of the beams that were strengthened under external load action was higher than that of the beams that were strengthened without external load action. Experimental research indicated that after a 135-d long-term load action, the deflections became similar (4.33 mm) (Fig. 5). Deformations in the tensioned layers and longitudinal shear deformations in the concrete and carbon fibre composite interface were also similar (Fig. 6).

The deflection evolution of the strengthened beams when the external load was decreased is presented in Fig. 7. The first point corresponds to the moment when a long-term load level of the non-strengthened beams was reached; the second and third points occur when the long-term load level of the non-strengthened beams increased to 86%; the fourth and fifth points occurred when the long-term load level of the non-strengthened beams decreased to 52%; the sixth point occurred when the beams were strengthened with an external CFRP layer; and, the seventh point occurred when the load increased to 60% of the resistance of the strengthened beams.

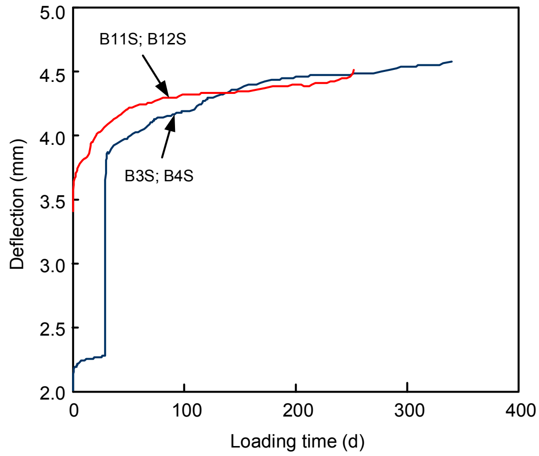

Fig. 5 Deflection of strengthened beams B3S, B4S, B11S, and B12S

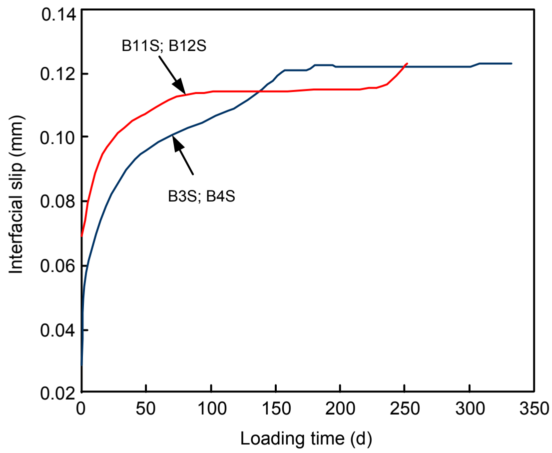

Fig. 6 Slip of the external carbon fibre composite layer of beams B3S, B4S, B11S, and B12S

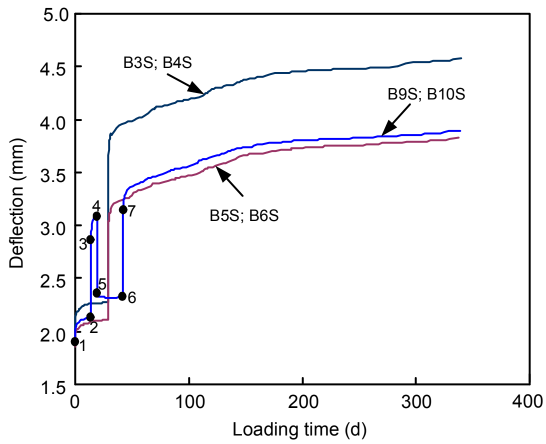

Fig. 7 Deflection of strengthened beams B3S, B4S, B5S, B6S, B9S, and B10S

Additional anchorage of the external carbon fibre composite layer increases the stiffness of concrete and carbon fibre composite interface (Fig. 4), and decreases the initial deflection of the strengthened beams. Therefore, the deflection during the long-term load action was lower when additional CFRP laminate was used as an anchor (Fig. 8). When the external carbon fibre composite layer was additionally anchored with carbon fibre clamps, the deflection of beams B9S and B10S during the first 100 d of the long-term load action was 2.1 times lower than that of the beams where additional anchorage was not used. Beams anchored with additional steel plates or steel clamps had little change in deflection. When additionally anchored with steel clamps, the deflection was 1.77 times lower, and when additionally anchored with steel plates, the deflection was only 1.19 times lower than that in the beams where the external composite layer was not additionally anchored.

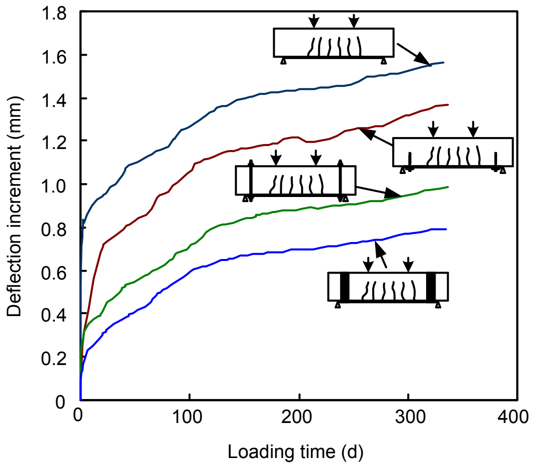

Fig. 8 Deflection of the strengthened beams when different additional anchorage methods are used

At the end of the long-term load action (i.e., after 330 d), the deflection increment of the strengthened beams when the external composite layer was not additionally anchored reached 1.562 mm. The deflection increment of the strengthened beams when the external layer was additionally anchored with steel plates was 1.366 mm; when the strengthened beams were additionally anchored with steel clamps or carbon fibre clamps, the deflection increment was 0.98 mm and 0.795 mm, respectively. It was experimentally determined that deflection increment at the end of the experiment when carbon fibre clamps were used was 1.96 times lower than that of the beams without additional anchors to the external layer. When steel clamps were used, it was 1.59 times lower; when steel plates were used, it was 1.14 times lower.

Experimental research showed that the most effective strengthening was achieved when carbon fibre composite clamps were used. Carbon fibre clamps glued around the whole section can effectively decrease longitudinal slip of the CFRP (Fig. 4).

6 Comparison of experimental and calculated deflection results

Using the proposed calculation methodology, the deflection of the strengthened beams under the influence of a long-term load was calculated. The calculated deflections and their comparison with experimental values are presented in Table 4. The calculation results were also compared with the experimental results published by other researchers. The reinforced concrete beams used by Tan and Saha (2006) were strengthened with glass fibre reinforced polymer, and additional anchorage with GFRP clamps was used. Al Chami *et al.* (2009) used reinforced concrete beams strengthened with carbon fibre reinforced polymer, and no additional anchorage was used. Deflections of the strengthened beams were calculated at different time intervals (long-term load action at intervals of 100 and 300 d). The change in creep deformations in the compression zone was evaluated according to the proposed calculation methodology as shown in Eq. (9) or Eq. (14). The stiffness of the concrete and CFRP interface depends on various factors, such as tensioned concrete deformation characteristics, concrete cracking level, adhesive characteristics, and load level. The influence of interface stiffness for beam deflection was evaluated using the effective shear modulus.

The regression analysis of the experimental results was used to determine the effective shear modulus of the concrete and carbon fibre composite interface:

$$G_{\mathrm{c,eff}}(t)=2.34E_{\mathrm{c,eff}}(t)+8.31\frac{\mu_{\mathrm{s1}}}{\mu_{\mathrm{f}}}+11.04\frac{M_{\mathrm{e}}}{M_{\mathrm{r,s}}k_{\mathrm{a}}}, \tag{26}$$

Table 4 Comparison of experimentally determined and calculated deflections of strengthened beams at different time intervals

Beam		Deflection (mm)								
		0 d			100 d			300 d		
		$\omega_{v,exp}$	$\omega_{v,cal}$	$\omega_{v,exp}/\omega_{v,cal}$	$\omega_{v,exp}$	$\omega_{v,cal}$	$\omega_{v,exp}/\omega_{v,cal}$	$\omega_{v,exp}$	$\omega_{v,cal.}$	$\omega_{v,exp}/\omega_{v,cal}$
This study	B3S	2.79	3.37	0.881	4.04	4.66	0.867	4.33	5.07	0.854
	B4S	3.28		0.973	4.57		0.981	4.80		0.947
	B5S	2.87	2.97	0.966	3.57	3.86	0.925	3.76	4.00	0.940
	B6S	2.87		0.966	3.61		0.935	3.86		0.965
	B7S	5.09	5.17	0.985	6.12	6.16	0.994	6.40	6.51	0.983
	B8S	4.08		0.789	5.19		0.843	5.40		0.829
	B9S	3.01	3.41	0.883	3.56	4.08	0.873	3.71	4.18	0.888
	B10S	3.25		0.953	3.89		0.953	4.08		0.976
	B11S	3.35	3.57	0.938	4.21	4.66	0.903			
	B12S	3.48		0.975	4.43		0.951			
Tan and Saha (2006)	GB1-49	5.5	5.63	0.977	7.6	7.82	0.972	8.1	8.29	0.977
	GB1-59	7.0	7.24	0.967	10.0	10.15	0.985	10.8	12.11	0.892
	GB1-70	8.5	8.70	0.977	11.1	11.80	0.941	12.8	13.38	0.957
	GB3-40	4.5	4.77	0.943	6.1	6.48	0.941	6.9	7.17	0.962
	GB3-49	5.7	5.93	0.961	8.5	8.65	0.983	9.1	9.35	0.973
	GB3-59	7.7	8.02	0.960	10.4	10.60	0.981	11.6	11.94	0.972
Al Chami *et al.* (2009)	1M10	7.9	8.10	0.975	10.5	10.92	0.962			
	2M10	7.8	8.12	0.961	10.7	11.05	0.968	12.4	12.81	0.968
	2M10	11.0	11.21	0.981	16.0	16.65	0.961	19.0	19.93	0.953
	2M15	7.1	7.54	0.942	10.4	10.69	0.973	12.3	12.85	0.957
	2M15	8.2	8.40	0.976	12.6	12.89	0.978	15.2	15.89	0.957

where k_a is a coefficient that indicates the additional anchorage method for a carbon fibre composite layer. When the carbon fibre composite layer does not have additional anchors, then k_a=1 when the anchors are placed under supports or pressed with an anchored steel plate, k_a=0.9 when metal clamps are used as additional anchors, k_a=0.7 when carbon fibre clamps are used as additional anchors, k_a=0.65.

A comparison of the experimental and calculated deflection results showed that the calculated results of the beams without additional anchorage were approximately 5% higher than those of the experimental ones. The calculated deflections of the beams with an external layer with additional anchors are approximately 6% higher than those of the experimental ones.

7 Conclusions

The change in longitudinal shear creep deformations in the interface of concrete and CFRP and the evolution of creep deformations in the compression zone influenced the deflection of strengthened beams.

Deflection analysis based on the built-up-bars theory is proposed in this paper. According to the proposed method, deflection can be calculated by accounting for the partial interface stiffness of the strengthened reinforced concrete member and carbon fibre composite, the creep deformations of the concrete compression zone and cracking of the tension zone of the strengthened reinforced concrete member.

The experimental results showed that longitudinal shear creep deformations developed during a long-term load action in the interface of the strengthened flexural reinforced concrete member and carbon fibre composite. After a 330-d long-term loading, the slip of the CFRP layer increased 12 times. An increase in the longitudinal shear deformations and creep deformations in the compression zone caused deflection to increase up to 52% during this time period.

The results suggest that the additional anchorage of carbon fibre composite by steel plates, by steel clamps, or by carbon fibre clamps resulted in reduced longitudinal shear creep deformations and, consequently, in reduced deflection. The most effective strengthening was obtained using carbon fibre clamps. When the composite layer was additionally anchored with carbon fibre clamps, the slip of the composite layer at the end of the test (i.e., after 330 d), was reduced by 5.1 times compared with the case when the external layer was not additionally anchored. By comparison, for the beams with the composite layer additionally anchored by steel plates and by steel clamps, the length of the slip decreased 1.5 and 1.6 times, respectively.

Deflection for the beams with the composite layer additionally anchored by carbon fibre clamps at the end of the long-term test of 330 d was 1.96 times lower than that for the beams without an additional anchorage of the composite layer. When the composite layer was additionally anchored by steel plates or by steel clamps, the deflection was 1.14 or 1.59 times lower, respectively.

The analysis of theoretical and experimental deflection values showed that deflection values determined by the proposed method agreed sufficiently well with those determined by all test results in Table 4.

Acknowledgements

Experiments were carried out in the Structures Research Laboratory at Civil Engineering Research Center of Vilnius Gediminas Technical University, Lithuania.

References

Al Chami, G., Theriault, M., Neale, K.W., 2009. Creep behaviour of CFRP-strengthened reinforced concrete beams. *Construction and Building Materials*, **23**(4):1640-1652. [doi:10.1016/j.conbuildmat.2007.09.006]

Balevičius, R., Dulinskas, E., 2010. On the prediction of non-linear creep strains. *Journal of Civil Engineering and Management*, **16**(3):382-386. [doi:10.3846/jcem.2010.43]

Benyoucef, S., Tounsi, A., Adda Bedia, E.A., Meftah, S.A., 2007a. Creep and shrinkage effect on adhesive stresses in RC beams strengthened with composite laminates. *Composites Science and Technology*, **67**(6):933-942. [doi:10.1016/j.compscitech.2006.07.007]

Benyoucef, S., Tounsi, A., Benrahou, K.H., Adda Bedia, E.A., 2007b. Time-dependent behavior of RC beams strengthened with externally bonded FRP plates: interfacial stresses analysis. *Mechanics of Time-Dependent Materials*, **11**(3-4):231-248. [doi:10.1007/s11043-007-9045-2]

Benzaid, R., Chikh, N.E., Mesbah, H., 2008. Behaviour of square concrete column confined with GFRP composite wrap. *Journal of Civil Engineering and Management*, **14**(2):115-120. [doi:10.3846/1392-3730.2008.14.6]

Dai, J., Ueda, T., Sato, Y., 2005. Development of the nonlinear bond stress-slip model of fiber reinforced plastic sheet-concrete interfaces with a simple method. *Journal of Composites for Construction*, **9**(1):52-62. [doi:10.1061/(ASCE)1090-0268(2005)9:1(52)]

Davis, G.D., Rich, M.J., Drzal, L.T., 2004. Monitoring moisture uptake and delamination in CFRP-reinforced concrete structures with electrochemical impedance sensors. *Journal of Nondestructive Evaluation*, **23**(1):1-9. [doi:10.1023/B:JONE.0000045216.94094.f5]

Diab, H., Wu, Z., Iwashita, K., 2009. Short and long-term bond performance of prestressed FRP sheet anchorages. *Engineering Structures*, **31**(5):1241-1249. [doi:10.1016/j.engstruct.2009.01.021]

EN 1992-1, 2001. Eurocode 2: Design of Concrete Structures. Part 1: General Rules and Rules for Buildings. Brussels, Belgium.

Ferrier, E., Hamelin, P., 2002. Long-time concrete-composite interface characterization for reliability prediction of RC beam strengthened with FRP. *Materials and Structures*, **35**(9):564-572. [doi:10.1007/BF02483125]

Ferrier, E., Michel, L., Jurkiewiez, B., Hamelin, P., 2010. Creep behavior of adhesives used for external FRP strengthening of RC structures. *Construction and Building Materials*, **25**(2):461-467. [doi:10.1016/j.conbuildmat.2010.01.002]

Fib Task Group 9.3, 2001. Externally Bonded FRP Reinforcement for RC Structures. Fib Bulletin 14, Lausanne, Switzerland, p.130.

Gao, B., Kim, J.K., Leung, C.K.Y., 2003. Effect of rubber modifier on interlaminar fracture toughness of CFRP-concrete interface. *Composites Science and Technology*, **63**(6):883-892. [doi:10.1016/S0266-3538(02)00311-1]

Kim, Y.J., Wight, R.G., Green, M.F., 2008a. Flexural strengthening of RC beams with prestressed CFRP sheets: Development of nonmetallic anchor systems. *Journal of Composites for Construction*, **12**(1):35-43. [doi:10.1061/(ASCE)1090-0268(2008)12:1(35)]

Kim, Y.J., Wight, R.G., Green, M.F., 2008b. Flexural strengthening of RC beams with prestressed CFRP sheets:

Using nonmetallic anchor systems. *Journal of Composites for Construction*, **12**(1):44-52. [doi:10.1061/(ASCE)1090-0268(2008)12:1(44)]

Lee, Y.J., Boothby, T.E., Bakis, C.E., Nanni, A., 1999. Slip modulus of FRP sheets bonded to concrete. *Journal of Composites for Construction*, **3**(4):161-167. [doi:10.1061/(ASCE)1090-0268(1999)3:4(161)]

Livshyc, J.D., 1976. Calculation of Reinforced Concrete Structures with Evaluation of Concrete Shrinkage and Creep. Golovnoe Izdatelstvo Kiev, Russia (in Russian).

Marchukaitis, G., Valivonis, Yu., Bareishis, J., 2007. An analysis of the joint operation of a CFRP concrete in flexural elements. *Mechanics of Composite Materials*, **43**(5):467-478. [doi:10.1007/s11029-007-0044-9]

Marčiukaitis, G., Jonaitis, B., Valivonis, J., 2006. Analysis of deflections of composite slabs with profiled sheeting up to the ultimate moment. *Journal of Constructional Steel Research*, **62**(8):820-830. [doi:10.1016/j.jcsr.2005.11.022]

Marčiukaitis, G., Daugevičius, M., Valivonis, J., 2010. The fragmentation of the tensioned zone of the strengthened reinforced concrete beam with carbon fiber composite. *Engineering Structures and Technologies*, **2**(4):129-137 (in Lithuanian). [doi:10.3846/skt.2010.17]

Rzhanitsyn, A.R., 1986. Built-up Bars and Plates. Strojizdat, Moscow, Russia (in Russian).

Skuturna, T., Valivonis, J., Vainiūnas, P., Marčiukaitis, G., Daugevičius, M., 2008. Analysis of deflections of bridge girders strengthened by carbon fibre reinforcement. *The Baltic Journal of Road and Bridge Engineering*, **3**(3):145-151. [doi:10.3846/1822-427X.2008.3.145-151]

Tan, K.H., Saha, M.K., 2006. Long-term deflections of reinforced concrete beams externally bonded with FRP system. *Journal of Composites for Construction*, **10**(6):474-482. [doi:10.1061/(ASCE)1090-0268(2006)10:6(474)]

Valivonis, J., 2006. Analysis of behaviour of contact between the profiled steel sheeting and the concrete. *Journal of Civil Engineering and Management*, **12**(3):187-194.

Wang, W., Li, G., 2006a. Experimental study and analysis of RC beams strengthened with CFRP laminates under sustaining load. *International Journal of Solids and Structures*, **43**(6):1372-1387. [doi:10.1016/j.ijsolstr.2005.03.076]

Wang, W., Li, G., 2006b. Experimental study of RC beams strengthened with CFRP sheets under sustaining loads. *Journal of Wuhan University of Technology-Materials Science Edition*, **21**(3):82-85. [doi:10.1007/BF02840887]

Wang, W., Dai, J., Li, G., Huang, C., 2011. Long-term behavior of prestressed old-new concrete composites beams. *Journal of Bridge Engineering*, **16**(2):275-285. [doi:10.1061/(ASCE)BE.1943-5592.0000152]

Weimer, C., Haupert, F., 2000. Influence of aggregate structure on mode-III interfacial fracture between concrete and CFRP. *Applied Composite Materials*, **7**(2-3):183-193. [doi:10.1023/A:1008967723065]

Xiong, G.J., Jiang, X., Liu, J.W., Chen, L., 2007. A way for preventing tension delamination of concrete cover in midspan of FRP strengthened beams. *Construction and Building Materials*, **21**(2):402-408. [doi:10.1016/j.conbuildmat.2005.08.005]